Expanded View Figures

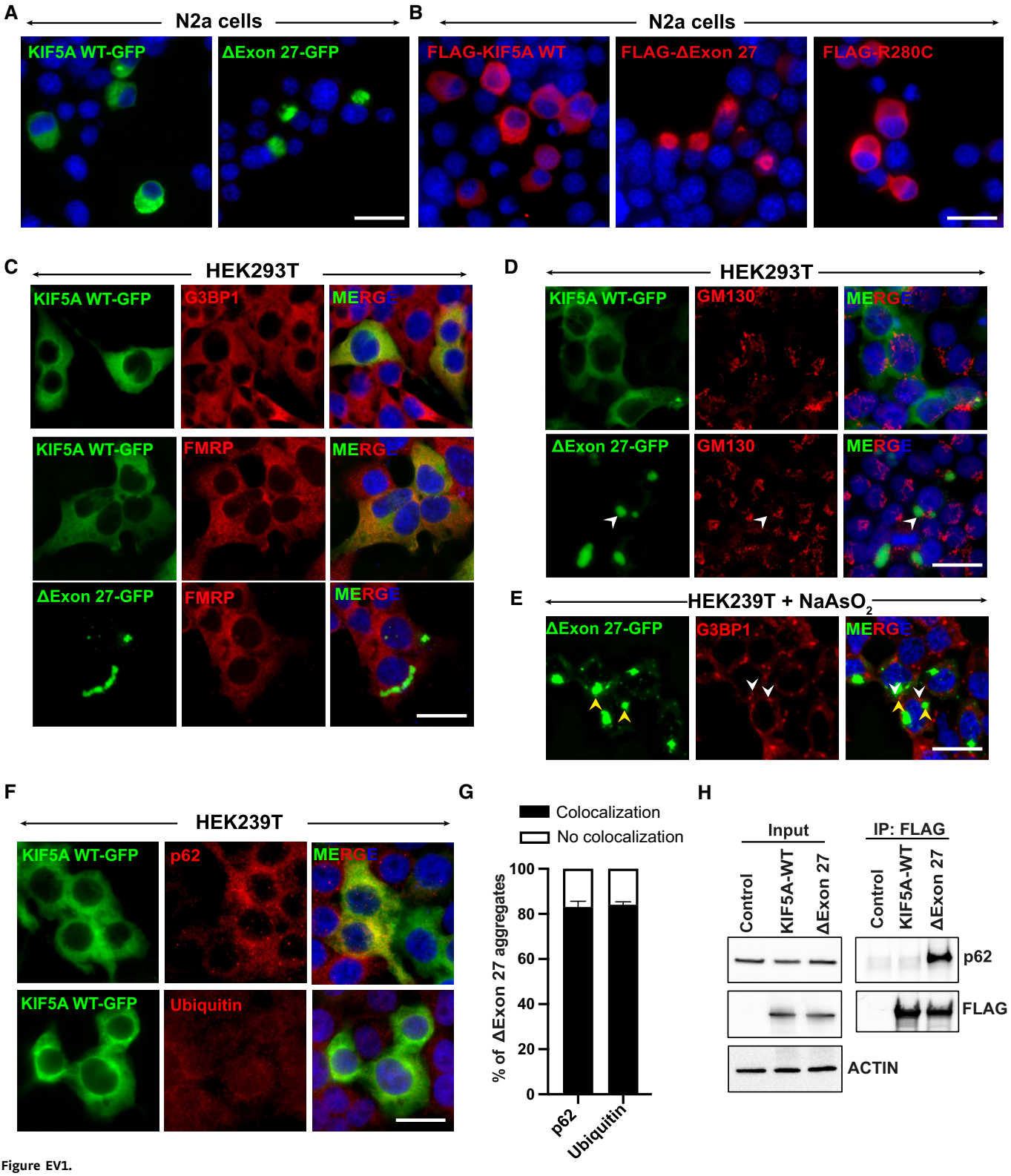

Figure EV1.

Figure EV1. KIF5A ΔExon27 is prone to form cytoplasmic aggregates.

A, B Expression of human KIF5A WT and disease-associated mutants with C-terminal GFP (A) or N-terminal FLAG (B) tags in N2a cells. Scale bar: 20 μm.
C Colocalization of G3BP1 and FMRP, markers of stress granules, with KIF5A WT or ΔExon27 expressed in HEK293T cells. Scale bar: 20 μm.
D GM130 (a Golgi marker) staining in HEK293T cells expressing either KIF5A WT or ΔExon27. Scale bar: 20 μm.
E G3BP1 staining in HEK239T cells expressing ΔExon27 and treated with sodium arsenite (200 μM) for 30 min. White and yellow arrowheads highlight stress granules and ΔExon27 aggregates respectively. Scale bar: 20 μm.
F p62 and ubiquitin staining in KIF5A WT expressing HEK293T cells. Scale bar: 20 μm.
G Percent of cells with p62 and ubiquitin colocalized with cytoplasmic ΔExon27 granules. Bars indicate mean ± SD.
H Immunoprecipitation of KIF5A using antibodies against the N-terminal FLAG tag also pulled down endogenous p62 only in cells expressing Δexon27, but not WT KIF5A. Three biological replicates, $n = 200$ cells per experiment.

Figure EV2. KIF5A ΔExon27 accumulates at the plus-ends of microtubules.

A Staining of TDP-43 in HEK293T cells expressing either KIF5A WT or ΔExon27 showed nuclear TDP-43. Three biological replicates, $n = 200$ cells per experiment. Scale bar: 20 μm.
B Western blot detecting KIF5A expression with transient transfection and lentiviral transduction. Two biological replicates.
C ΔExon27 expressed in HEK293T cells via lentiviral transduction forms small aggregates that colocalize with p62 (white arrowhead). Two biological replicates. Scale bar: 20 μm.
D Colocalization of p62 with KIF5A ΔExon27 granules. Scale bar: 20 μm.
E Mitochondria distribution in primary cortical neurons expressing KIF5A WT or ΔExon27. Scale bar: 20 μm.
F Expression of KIF5A WT-mApple and Δexon27-mApple in LLC-PK1 cells stably expressing tubulin-GFP. KIF5A Δexon27 shows aggregates at proximal tubule regions as highlighted by the white arrowhead. Scale bar: 20 μm.
G Δexon27 expressed in LLC-PK1 cells shows aggregates that colocalize with microtubule plus-end-tracking protein EB1 at the proximal extrusions. Three biological replicates, $n = 30$ cells per experiment. Scale bar: 20 μm.

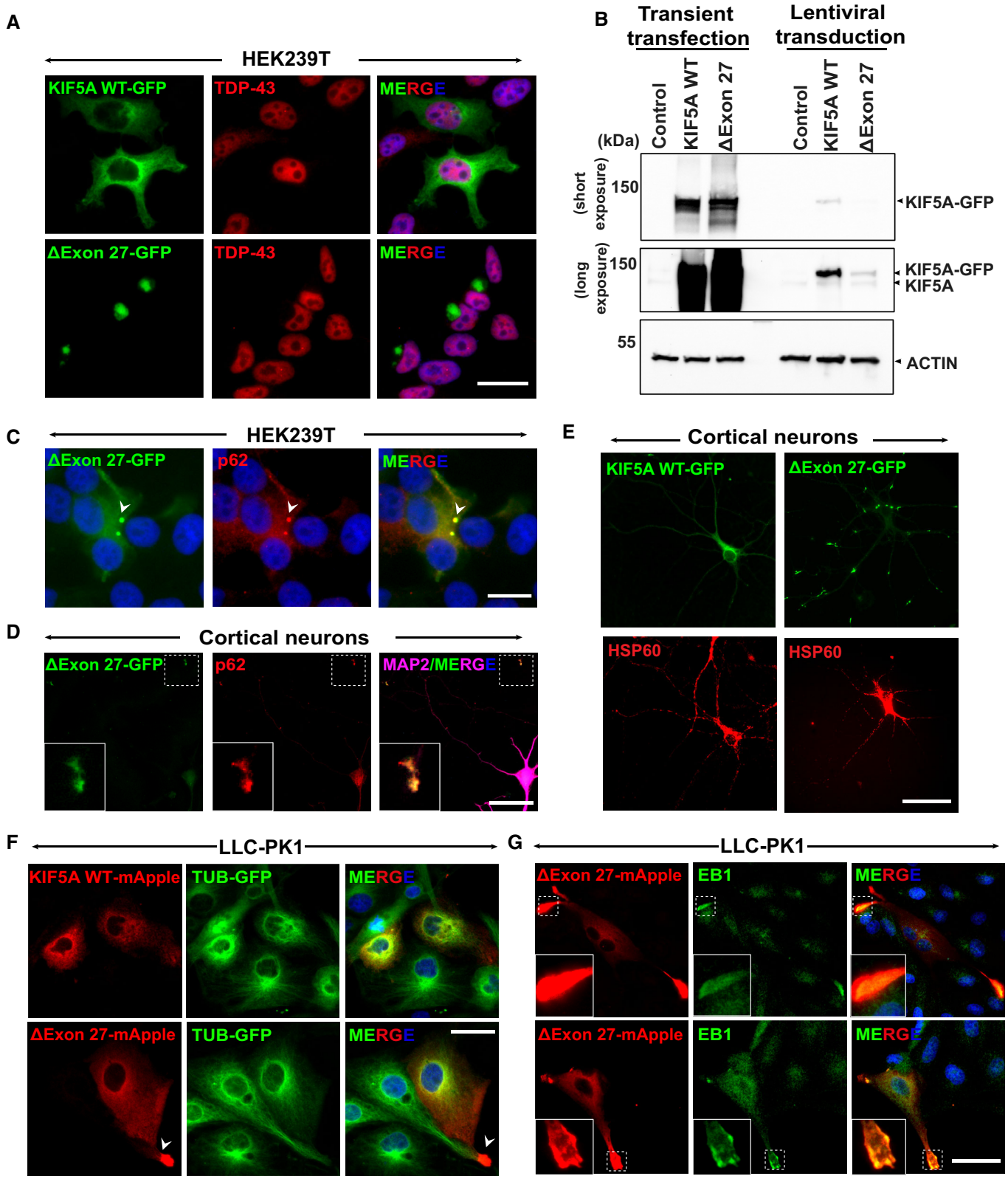

Figure EV2.

Figure EV3. Motile properties of KIF5A ΔExon27 and characterization of truncation mutants K998 and ΔC.

A Schematic illustrations of KIF5A truncation mutants, K998 and ΔC.

B Both KIF5A K998 and ΔC truncated proteins diffuse in the cytoplasm when expressed in HEK293T and N2a cells. Two biological replicates, $n = 100$ cells per experiment. Scale bar: 20 μm.

C Motor landing rate of KIF5A ΔExon27 along the microtube was accessed. ΔExon27 does not have a preference over the landing location on microtubules.

D Motor velocities (middle) and run-lengths (right) were determined based on kymographs (example on the left) for KIF5A WT and ΔExon27 complexes. HEK293T cells were transfected with both KIF5A WT-GFP and ΔExon27-mApple. The movements of WT and ΔExon27 were assessed by tracking either GFP or mApple, respectively. The right kymograph in *D* is the overlay of the GFP and mApple of moving WT-GFP/ΔExon27-mApple complexes. The *x*-axis scale for the processivity graphs was limited to 20 μm to permit a direct comparison of the run-lengths of the different constructs. Diagonal lines in the kymograph represent KIF5A molecules moving over time. The velocity data were fit with Gaussian distribution and the processivity data were fit with an exponential decay function. The depicted scale bars for all kymographs shown in this figure is 5 μm (horizontal line) and 10 s (vertical line). The measured values for the velocities and run-lengths are listed in Table 1.

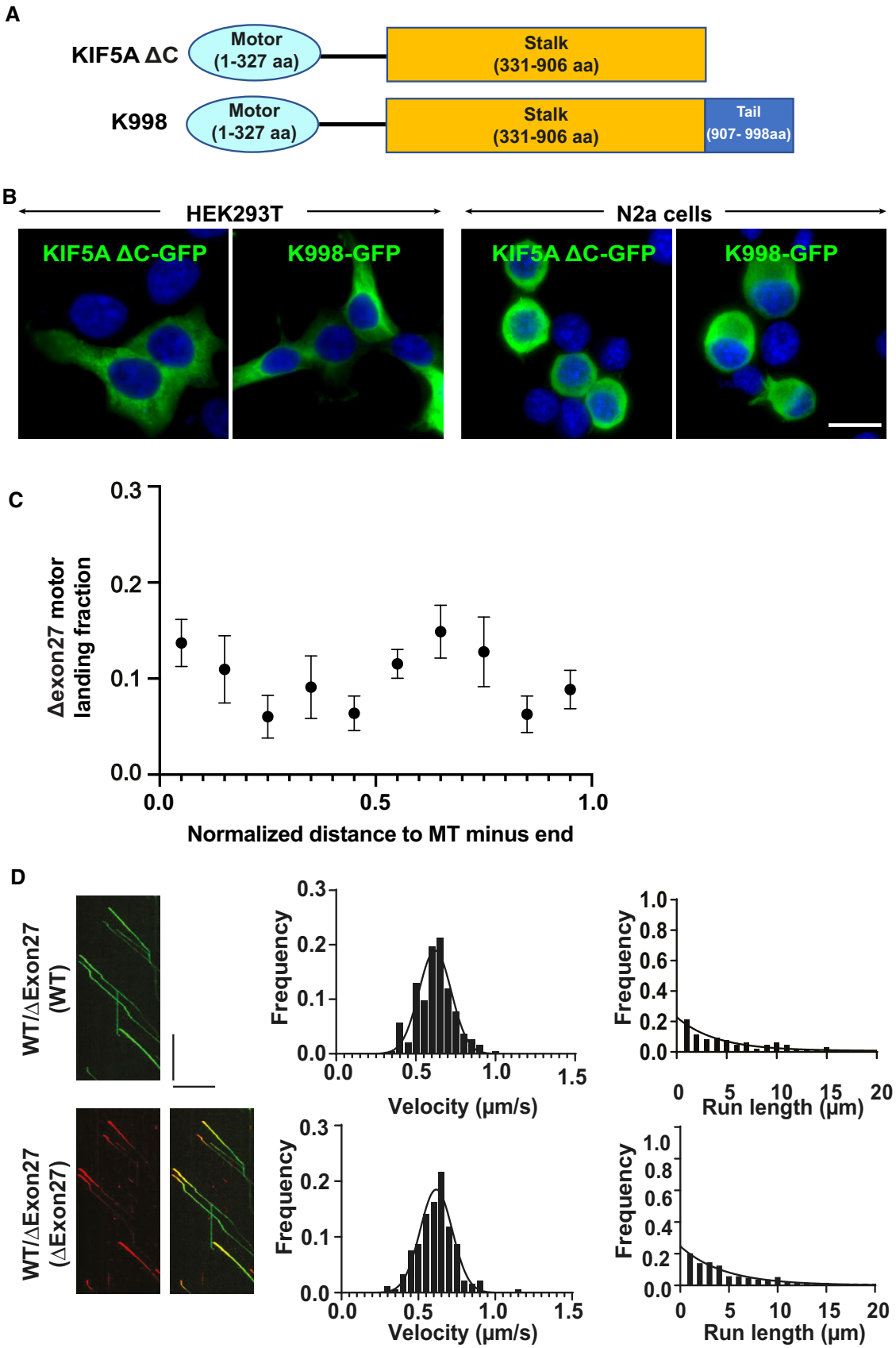
A
KIF5A ΔC
Motor (1-327 aa)
Stalk (331-906 aa)
K998
Motor (1-327 aa)
Stalk (331-906 aa)
Tail (907- 998aa)
B
HEK293T
N2a cells
KIF5A ΔC-GFP
K998-GFP
KIF5A ΔC-GFP
K998-GFP
C
Δexon27 motor landing fraction
Normalized distance to MT minus end
D
WT/ΔExon27 (WT)
WT/ΔExon27 (ΔExon27)
Frequency
Velocity (μm/s)
Run length (μm)

Figure EV3.

Figure EV4. Enhanced motor self-association in KIF5A ΔExon27.

A Histograms of the measured fluorescence intensities of the various moving kinesin motors. The fluorescence intensity in every frame of each moving spot was measured, accumulated, and plotted in a histogram. Numerous studies have shown that truncated kinesin-1 motors are dimeric and active (Friedman & Vale, 1999; Tomishige *et al*, 2006; Lam *et al*, 2021), and kinesin-1 family is highly conserved in the motor domain. Hence, a truncated KIF5A motor (K490, amino acid 1–490) was generated and used as the standard for fluorescence intensity of dimeric motors. Moving KIF5A ΔExon27 molecules exhibit a much larger fraction of motors with high fluorescence intensities. The majority of moving KIF5A ΔExon27 spots consist of multiple motors. K490: repeated two times, $n = 189$; other constructs are described in Fig. 4. Number of frames that have been analyzed: K490, $n = 1{,}953$; ΔC, $n = 2{,}964$; WT, $n = 1{,}634$; K998, $n = 5{,}462$; ΔExon27, $n = 8{,}345$.

B Two example traces of K490-EGFP showing photobleaching events. K490-EGFP was used as the standard dimer molecule to determine the fluorescent intensity of EGFP.

C Histogram of measured intensities of moving K490-EGFP molecules that showed a single photobleaching step. The intensity distribution was fit with two Gaussian functions, resulting in mean values of 145.5 ± 3.6 (mean ± SD) and 163.0 ± 7.3. With an average background fluorescence signal of 127.6 ± 0.7, one obtains an average fluorescent intensity is 17.7 for EGFP (in a.u.).

D, E Determination of the percentage of the number of motors for each motor complex. KIF5A K490 and KIF5A ΔExon27 are depicted here as examples (D). The same method was applied to the other motors. Each moving spot was assigned to a single intensity value that corresponded to the average intensity measured over the first 20 frames of the moving spot so the intensity would be less likely to be averaged down due to photobleaching. The measured values were then accumulated and plotted in a histogram. Based on the mean intensity of EGFP, the measured intensity values were sorted into intervals of 35.4 (depicted by the turquoise dashed lines), with the first interval centered at 163 (163 ± 17.7). The percentage of each bin was calculated and then assigned to the calculated number of dimers (E). The percentages of a single dimer for all KIF5A constructs are: K490, 100%; ΔC, 88%; K998, 54%; WT, 54%; ΔExon27, 25%.

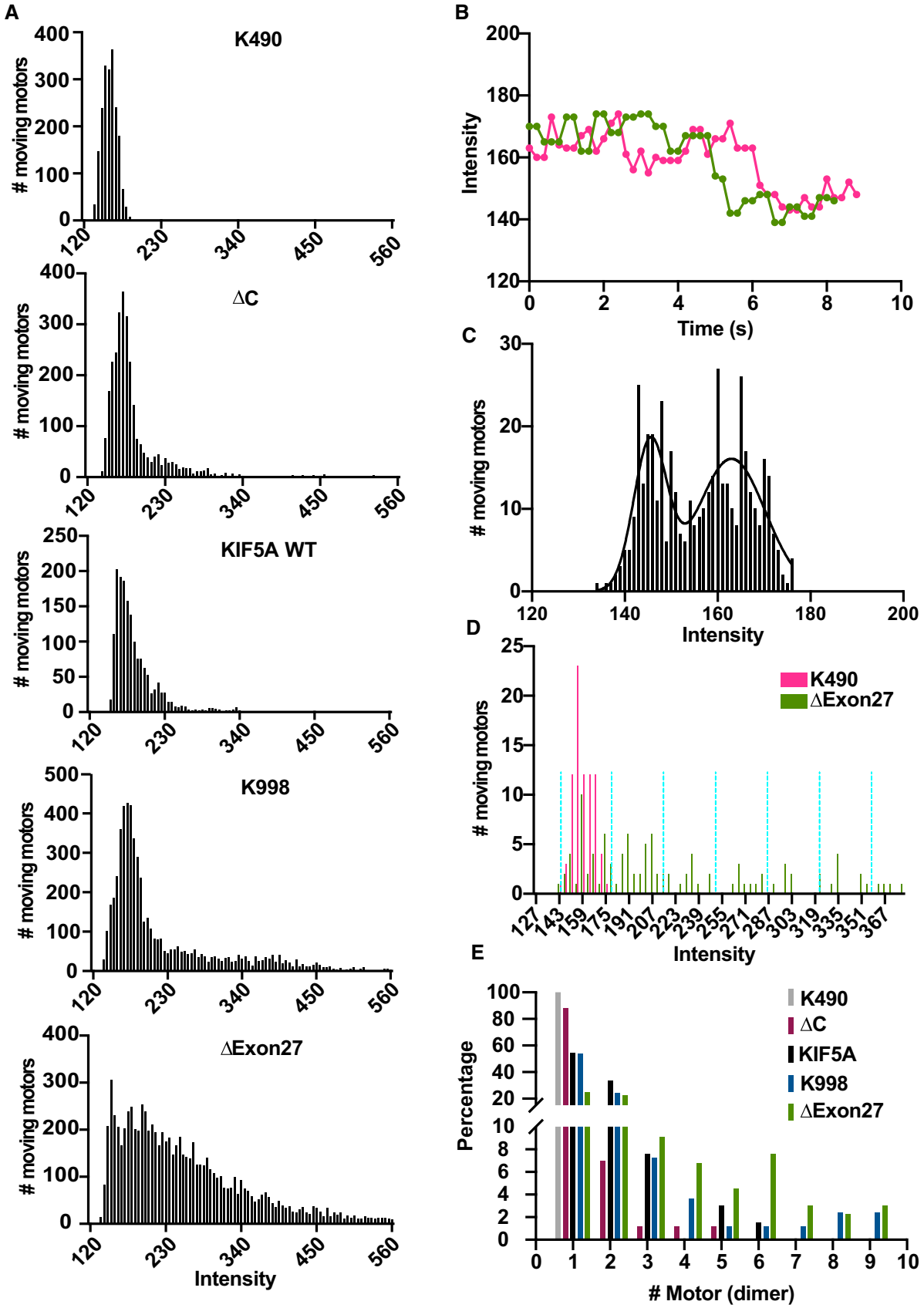
A
K490
ΔC
KIF5A WT
K998
ΔExon27
moving motors
Intensity
B
Intensity
Time (s)
C
moving motors
Intensity
D
K490
ΔExon27
moving motors
Intensity
E
K490
ΔC
KIF5A
K998
ΔExon27
Percentage
Motor (dimer)

Figure EV4.

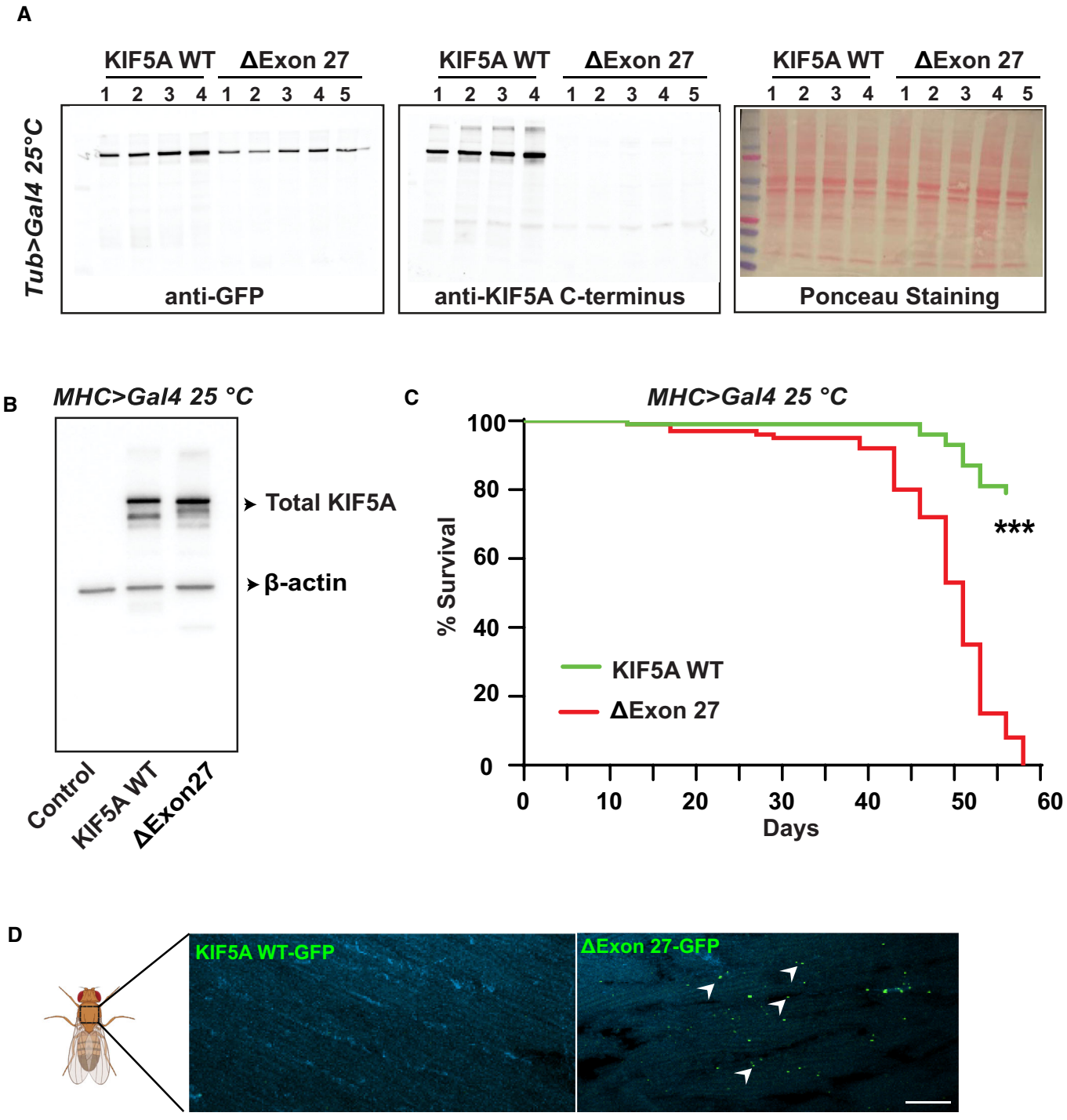

Figure EV5. Muscle-specific expression of ΔExon27 in *Drosophila* leads to early lethality.

A Western blot detecting the level of human KIF5A proteins in *Drosophila* ubiquitously expressing WT or ΔExon27 driven by tubulin-Gal4. Genotypes were: KIF5A WT (UAS-KIF5A WT-GFP/ tubulin-Gal4); ΔExon27 (UAS-ΔExon27-GFP/ tubulin-Gal4). Samples from 4 (WT) and 5 (ΔExon27) different induvial lines were assessed with similar results, two independent experiments.

B Western blot detecting the expression of human KIF5A proteins in *Drosophila* expressing WT or ΔExon27 in muscle tissues driven by MHC-Gal4. Genotypes were: Control (MHC-Gal4/+); KIF5A WT (UAS-KIF5A WT-GFP/MHC-Gal4); ΔExon27 (UAS-ΔExon27-GFP/MHC-Gal4), two independent experiments.

C Lifespan of male flies expressing KIF5A WT or ΔExon27 in muscles driven by MHC-Gal4 at 25°C (n = 50 flies per group, two independent experiment ***$P < 0.001$, log-rank test).

D Aggregates accumulate in thorax muscles at 7 days post-eclosion in flies expressing ΔExon27, but not in those expressing KIF5A WT, n = 10 flies per group. Scale bar: 10 μm.